# 4.22 MEASUREMENTS AND SIMULATIONS OF THE DISPERSION OF A PASSIVE TRACER IN A MOUNTAINOUS AREA

*Karine Sartelet[1], Takeshi Saito[1], Masatoki Suzuki[1] and Yoichi Ichikawa[2]*
[1]Japan NUS Co. Ltd (Janus). Tokyo, JAPAN
[2]Central Research Institute of Electric Power Industry (CRIEPI). Tokyo, JAPAN

## INTRODUCTION

The aim of this paper is to study the dispersion of a tracer in the presence of topography under different wind conditions. Measurements of the tracer PMCH ($C_7F_{14}$: Perfluoro-Methyl Cyclohexane) carried out around the CRIEPI's Akagi Testing Center are compared to an atmospheric dispersion code, Mercure. After presenting the field experiments, Mercure is briefly introduced. The data required as inputs are the topography over Akagi Testing Center, meteorological conditions (humidity, wind, temperature and turbulence profiles) and the tracer release features. Finally, measurements and Mercure's outputs are compared and discussed.

## FIELD EXPERIMENTS

Experiments are conducted at a region of about 3km east and 3km south around Akagi Testing Center (36°28' 11" N; 139°11' 19" E), both in January 2001 and 2002. The site, 290m above sea level (ASL), is located at the southern foot about 10km south of Mt. Akagi that has several peaks of 1565m to 1828m ASL. The terrain around the site is very complex.
The tracer concentrations used for comparisons concern four sets of measurements: measurements done between 3.30pm and 4.00pm on the 23rd January 2001 (run 1), between 4.00pm and 4.30pm on the same day (run 2), between 5.00pm and 5.30pm on the 23rd January 2002 (run 3) and between 5.30pm and 6.00pm on the same day (run 4). Meteorological observations were conducted by ultrasonic anemometer and by Doppler-Sodar. The release conditions and sampling conditions, as well as meteorological measurements are summarized in table 1. A more detailed description of the field experiments is in Ichikawa (2003).

*Table 1. Outline of Tracer Emission and Sampling, and of meteorological measurements at the Akagi Testing Center experiment*

| Release height | 95 m ground level (GL) | Air flow rate | 0.035 $Nm^3$ /min |
|---|---|---|---|
| Tracer's flow rate | 90 g/h | Sampling time and rate | Every 30 minutes, 100ml/min |
| Conditions | Weather: no precipitation; wind direction: north (2001), west (2002); atmospheric stability: neutral | | |
| Ultrasonic anemometer sampled at 20Hz | Measurements of temperature and horizontal and vertical velocities at 100 m (GL). | | |
| Doppler-Sodar | Observation heights: 11 ground levels between 30m and 250m; Measurements of standard deviation of vertical wind velocity (2001), and standard deviation of horizontal and vertical wind velocities (2002) | | |

## MODELING: ASSUMPTIONS AND INPUT PARAMETERS

### Description of Mercure

Mercure is a computational fluid dynamic code (CFD), adapted to the atmosphere, which resolves the Navier-Stokes equations using the finite-difference and finite-volume fractional time step method, in three-dimensional domains. The flow is considered as non-isothermal, anelastic, and potential temperature is transported. The turbulence closure scheme used in these simulations is the standard $k-\varepsilon$ model. To account for the presence of topography, terrain-following curvilinear coordinates are used. The topography of Akagi Testing Center is quite complex and so induces large angles in some mesh cells, which alters the orthogonal structure of the mesh. Therefore, "pressure non-orthogonality terms" are taken into account in the set of equations solved. Further details about Mercure may be found in Rabillard et al. (1997).

**Input data**

To compare computed tracer concentrations to data, two sets of simulations are performed. The first simulation starts at 3.00pm and finishes at 4.30pm on the 23$^{rd}$. The second simulation starts at 4.30pm and finishes at 6.00pm on the 23$^{rd}$. The results of the first half an hour of these simulations are not used for comparison purposes. However, the simulations are set to start half an hour earlier than required for comparisons purposes in order to make sure that the wind field computed is stabilized before starting comparisons.

The horizontal domain used in the simulations extends over 8km x 8km in the horizontal, and to 4km height in the vertical. The topography over Akagi Testing Center is described in figure 1, the mesh (figure 2) uses 69 x 69 points in the horizontal and 49 points in the vertical. The time step used in the simulation is equal to 2s.

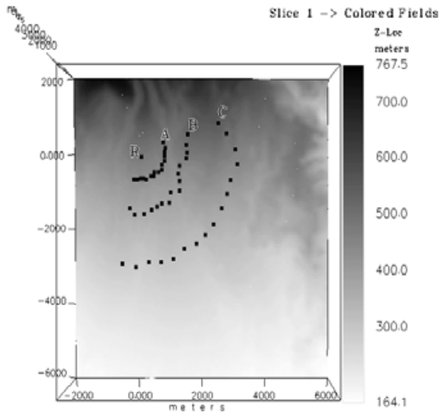


*Figure 1. Topography over Akagi Testing Center (southern foot of Mt. Akagi). The dots denote the positions of sensors. In the figure, the dot denoted "R" corresponds to the release point. The arc of dots denoted "A" corresponds to the arc of sensors that is the closest from the release point, while the arc denoted "C" corresponds to the arc that is the furthest from the release point. Although the positions of sensors are slightly different in 2001 and in 2002, only the positions for 2001 are presented here.*

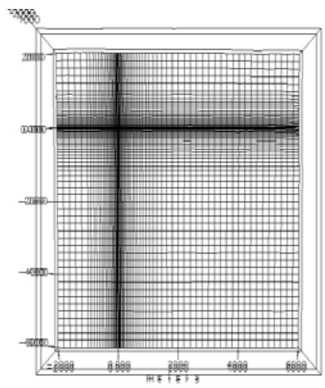

*Figure 2. Horizontal section of the mesh; the grid is refined around the release point (0, 0).*

The meteorological data required are humidity, wind, temperature and turbulence profiles.
The relative humidity is assumed to be constant in time and equal to 80%. The vertical profile of temperature $T$ is deduced from the temperature $T_0$ at the ground surface $T(z)=T_0-z\Gamma$, where $\Gamma$ is the adiabatic lapse rate and $z$ represents the vertical. The temperature $T_0$ at the ground surface is taken equal to 5ºC for runs 1 and 2 and to 3ºC for runs 3 and 4.

Wind speed V and turbulence (k, ε) profiles are deduced from wind data measured at 100m above ground surface (see figure 3), by an exponential low and a logarithmic law respectively:

$$V(z) = V_0 \left(z/z_0\right)^p \ , \ k(z) = U_m^2 \Big/ \sqrt{C_m} \ , \varepsilon(z) = U_m^3 \Big/ \left(K_m z\right) \qquad (1)$$

where $p = 0.15$ is an experimental constant, $z_0$ is the observational height (100m),
$K_m = 0.41$ is the Karman constant, $C_m = 0.09$ is an experimental constant,
$U_m = V_0 \, K_m / \log(z_0 / z_r)$ is the friction velocity with the roughness $z_r$ .

In Mercure, wind field is initialized in the whole computational domain using the vertical wind profile computed from the wind speed and direction measured at 100m above the ground. During the simulations, wind profiles are computed inside the computational domain using the wind data forced on the inlet lateral boundary conditions. The bottom boundary conditions chosen correspond to wall conditions with friction condition.

Winds measurements are performed at the release point every minute. However, because atmospheric wind velocity components vary very rapidly in both space and time, the mean velocity is explicitly resolved and the random component is represented using the standard $k-\varepsilon$ model. In the atmosphere, we generally consider that "standard" $k-\varepsilon$ is well fitted to describe data averaged over 10min. The wind speeds and directions used for initial and lateral boundary conditions are shown in figure 3.

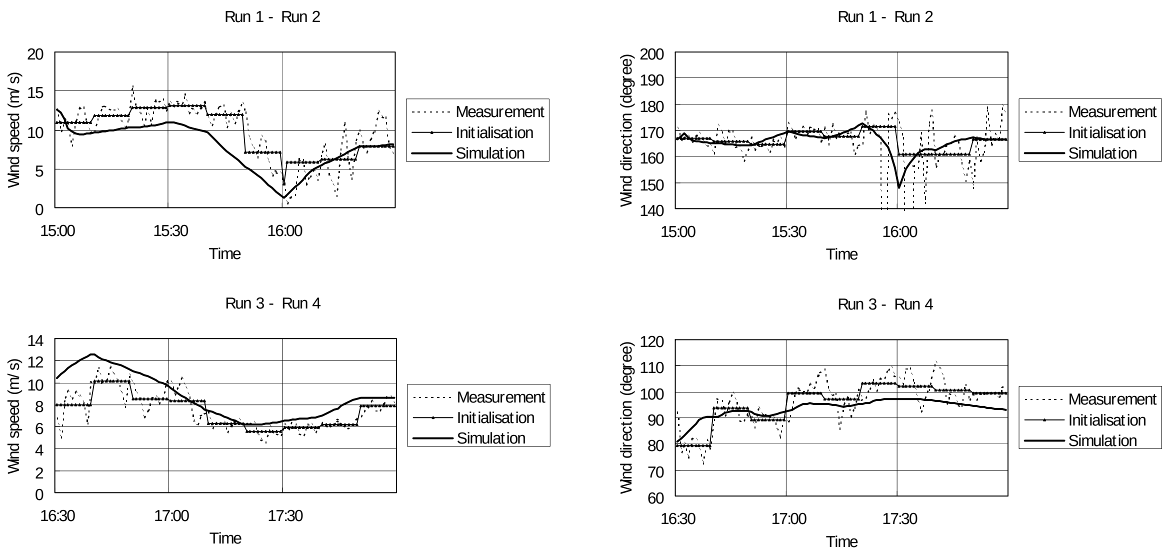


*Figure 3. Comparisons of wind speeds and directions at the release point at 100m height. The "initialization" profile corresponds to the profile used for initialization and lateral boundary conditions. It is obtained by averaging over 10min wind measurements at the release point. Down-wind direction is measured clockwise from the North. ( 0º represents South wind.)*

The computational domain is limited by artificial boundaries on five sides (top of the domain and four lateral sides). These artificial boundaries may lead to the reflection and to the amplification of perturbations that are propagating towards the outside of the domain.
One way to attenuate these perturbations is to define absorbing layers on the lateral sides and at the top of the domain. In these absorbing layers, the horizontal diffusivity coefficient is progressively increased. The thickness of the absorbing layers is set to five grid points in the horizontal and eight grid points in the vertical.

## RESULTS

### Wind field

Horizontal components of wind velocities are initialized in the whole domain using the measurements of wind speeds and directions obtained at 100m at the release point and averaged over 10min.

These measurements, averaged over 10min, are also used as lateral boundary conditions during the simulations. To check the consistency of the simulations, computed wind profiles at the release point are compared to measurements in figure 3.

### Tracer concentrations

Comparisons of tracer computed and measured concentrations at each arc are shown in figure 4. In order to quantify the comparisons, table 2 displays the mean-square root $\sigma$ and the peak accuracy prediction $\tau$ of the results, which are computed for each run as follows

$$\sigma^2 = \frac{1}{3}\sum_{j=1}^{3}\frac{\sum_i \left(M_{i,j} - C_{i,j}\right)^2}{\sum_i M_{i,j}^{\ 2}}, \quad \tau = \frac{1}{3}\sum_{j=1}^{3}\frac{\left|Max_i M_{i,j} - Max_i C_{i,j}\right|}{Max_i M_{i,j}} \qquad (2)$$

where $j$ corresponds successively to arc A, arc B and arc C, $i$ varies between 1 and the number of sensors for each arc, $M_{i,j}$ is the PMCH concentration measured at sensor $i$ and arc $j$ and $C_{i,j}$ is the averaged PMCH concentrations computed at the location of sensor $i$ and arc $j$. As shown in table 2 and figure 4, for run 4 at arc A, the computed concentration is about 4 times higher than the measured concentrations. However, in all other cases, the computed and measured concentrations are in excellent agreement.

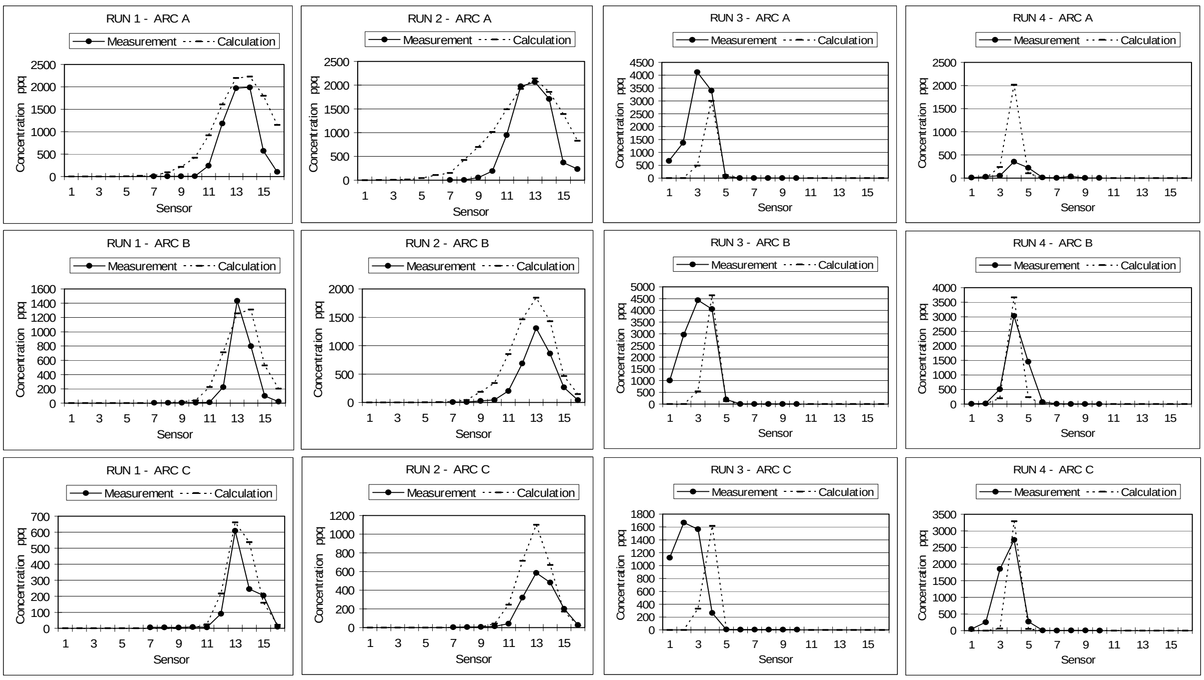


*Figure 4. Comparisons of tracer computed and measured concentrations at each arc and for each run (run 1, run 2, run 3 and run 4).*

*Table 2. Mean-square root $\sigma$ and the peak accuracy prediction $\tau$ for runs 1 to 4.*

| | **Run 1** | **Run 2** | **Run 3** | **Run 4** |
|---|---|---|---|---|
| $\sigma$ | 0.54 | 0.71 | 0.85 | 2.31 |
| $\tau$ | 0.10 | 0.44 | 0.12 | 1.70 |

**Turbulent kinetic energy**

Measurements of turbulent kinetic energy at the release point, as obtained by a vertical Doppler-Sodar, are compared to turbulent kinetic energy obtained from the $k-\varepsilon$ computation in figure 5. In figure 5, the measurements' profiles correspond to the average of 4 measurements' profiles for runs 1 and 2, and to the average of 5 measurements' profiles for runs 3 and 4. The measured turbulent kinetic energy profiles are deduced from measurements of standard deviations of wind velocities. Because only vertical velocities are measured in runs 1 and 2 (table 1), turbulent kinetic energy is deduced from the standard deviation of the vertical velocity by assuming that turbulence is isotropic. Although the release point is located over mountainous terrain, comparisons of turbulent kinetic energy are relatively good for all runs. However, in run 1 and run 2, below 150m, the measured turbulent kinetic energy is lower than the computed turbulent kinetic energy. This discrepancy may be due to the fact that the measured profiles are deduced from the standard deviation of vertical velocity only, under the assumption of isotropic turbulence, which may not be valid close to the ground and in very stable conditions.

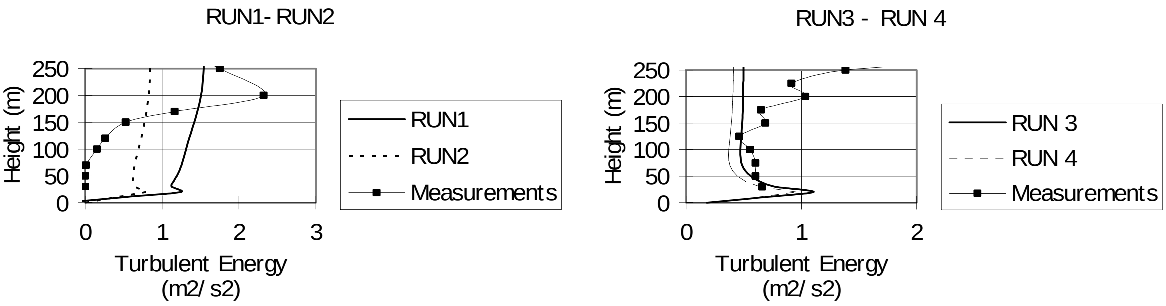


*Figure 5. Comparisons of measurements of turbulent energy to $k-\varepsilon$ model's predictions.*

**CONCLUSION**

Using a computational fluid dynamic code adapted to the atmosphere, Mercure, good agreements between measured and computed tracer concentrations have been obtained over Akagi Testing Center, stressing the adequacy of such a code to study dispersion of pollutants over complex terrain. Further studies may involve the use of more precise wind boundary conditions, which may be obtained by large-scale meteorological data or by wind field calculated over a larger site and by downscaling using a mass conservation model for example. Furthermore, as characteristics of turbulence depend on the closure scheme, it would be interesting to test other turbulence scheme than the standard $k-\varepsilon$ model to compare results with different turbulence closure schemes.

**REFERENCES**

*Rabillard, C., A. Albergel, T. Sevin, B. Carissimo, E. Dupont, L. Musson-Genon*, 1997: Recueil des fiches de validation du code MERCURE - Version 3.2. Rapport EDF, **HE-33/97/004**.

*Rabillard, C., B. Carissimo, E. Dupont,* 1997: Notice d'utilisation du code Mercure/ Mercure's users Guide - Version 3.3. Rapport EDF, **HE-33/97/003B**.

*Ichikawa, Y.*, 2003: Development of a method for predicting dispersion of exhaust gas from a low stack during downdraft. Komae Research Laboratory Report, **T02032**.